Recent Progress in Regulating Surface Potential for High Efficiency Perovskite Solar Cells

Jiaheng Nie [1], Yaming Zhang [2], Jizheng Wang [3], Lijie Li [4], and Yan Zhang [2,]*

[1] School of Cybersecurity (Xin Gu Industrial College), Chengdu University of Information Technology, Chengdu 610225, China

[2] School of Physics, University of Electronic Science and Technology of China, Chengdu 610054, China

[3] Beijing National Laboratory for Molecular· Sciences, CAS Key Laboratory of Organic Solids, Institute of Chemistry, Chinese Academy of Sciences, Beijing 100190, China

[4] College of Engineering, Swansea University, Swansea SA1 8EN, UK

Corresponding Author

***Yan Zhang** - *School of Physics, University of Electronic Science and Technology of China, Chengdu 610054, China*；https://orcid.org/0000-0002-7329-0382**.** Email: zhangyan@uestc.edu.cn

TOC GRAPHICS

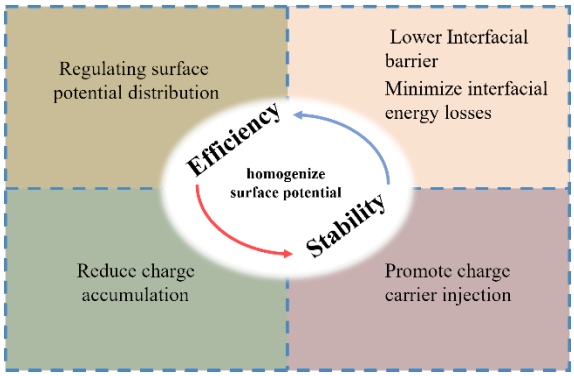

Perovskite solar cells (PSCs) have made remarkable progress in the past decade. The efficiency of single junction PSCs has now reached a record above 26% [1]. Tandem architectures can overcome the thermodynamic limits of single-junction cells, achieving efficiency of 32.5% [2]. Interface and surface modification are crucial for facilitating charge extraction, suppressing interfacial recombination, and increasing power conversion efficiency (PCE) and stability. Modulating perovskite surface energy to achieve uniform surface potential is beneficial to lower interfacial barriers, minimize interfacial losses, and enhance device efficiency [3-6].

Chen et al. modulated surface states by surface dipoles to form uniform surface potential distribution, achieving a record open-circuit voltage of 2.19 V [7]. Jiang et al. reduced potential fluctuations on perovskite thin film surfaces, boosting the efficiency of p-i-n perovskite solar cell devices by over 25% [3]. Detrimental surface treatments can make negative work function shifts, increasing carrier injection barriers, and enhancing ion migration and reducing device stability [3].

The interface between perovskite and indium tin oxide (ITO) requires potential well for improving the efficiency and stability of perovskite solar cells. The heterointerface between the

top perovskite surface and a charge-transport layer (CTL) needs no charge accumulation for both the hole-transport layer (HTL) and the electron-transport layer (ETL), which have a homogeneous electric-field distribution to avoid energy barrier or potential well. Regulating the surface potential distribution can change surface and interface barrier or potential well to minimize interfacial energy losses and promote charge carrier injection of interface.

Surface potential characterization can help to evaluate capacitive effects at the junction, impacting charge injection barriers and consequent device performance. The research progress in modulating the surface potential to enhance the efficiency and stability of devices is reviewed. Herein, it is discussed the performance enhancement of devices through polarization-induced surface potential modulation and outlined the future directions in polarization-modulated interfacial barriers. The uniformity of surface potential shows high open-circuit voltage (V_{OC}) and photoelectric conversion efficiency. The modulation of the surface potential can improve interfacial electric fields, forming favorable band bending, reducing series resistance, and promoting interfacial carrier extraction.

The techniques used to characterize interface potential including Kelvin probe force microscopy (KPFM), ultraviolet photoelectron spectroscopy (UPS), or transient surface photo-voltage (tr-SPV). KPFM has been widely performed on the surface potential distribution image of perovskite films or potential profile of cross-section in PSCs. UPS is used to characterize the energetic distribution of films or interface band alignment. The tr-SPV is used to study the concentration of separated charge carriers at each CTLs for studying charge extraction or recombination at interfaces.

Regulating surface potential in p-i-n perovskite solar cells. Inverted (p-i-n) structure perovskite solar cells exhibit higher stability, longer lifetimes, easily scalable fabrication, reliable operation, and compatibility with perovskite-based tandem device architectures, but have a lower device efficiency compared to typical n-i-p cells [4, 8, 9]. Tuning the surface potential of the top-surface region of perovskite layers can decrease the cross-interface recombination, by modifying interface band offset and decreasing minority carrier concentration of interface, cannot negatively affect the quality of bottom-surface region the perovskite film [10, 11].

Kelvin probe force microscopy (KPFM) map shown that the 1,3-propane-diammonium iodide (PDA) treatment significantly reduced the surface potential gradient with a typical standard deviation (σ) from 11.1 to 2.9 mV, as shown in fig. 1(a). The treated film is more homogeneous, and the interface recombination is decreased and carrier extraction is improved [4, 12]. Figure 1b shows the *J–V* curves of narrow band gap (NBG), wide band gap (WBG) and all-perovskite tandem devices, and stability measurement of WBG and all-perovskite tandem devices. PDA treatment make V_{OC} of WBG solar cells increase from 1.23 to 1.33 V, achieving PCE of 20.2% in WBG perovskite solar cell. PDA treatment reduced V_{OC} loss at the ETL from 104 to 16 mV without changing of HTL. The fabricated all-perovskite tandem solar cells shown V_{OC} of 2.19 V above previous highest reported V_{OC} of 2.13 V, and PCE of 27.4%.

Regulating surface potential induce diploes and n-type doping at the perovskite surface. Thus, the solar cells exhibited long device stability due to an increased ion migration barrier. The maximum power point (MPP) measurement shown that the PDA-treated WBG cell can operate for 700 h under 1 sun illumination without loss in PCE. Regulating surface potential may suppresses the halide segregation by involving a surface treatment removes or immobilizes surface defects.

Reactive surface engineering: Jiang et al. reported a reactive surface engineering approach by using 3-(aminomethyl)pyridine (3-APy) based post-growth treatment, for increasing efficiency of p–i–n PCSs to 25.37% [3]. The 3-APy process improved the device efficiency to 25.35% with highest V_{OC} of 1.19 V. Atomic force microscopy (AFM) and KPFM measurements of the surface morphology and potential distribution of the films show that clear grain boundary edges indicate a high crystallinity of the perovskite, as shown in fig. 2(a). Transient reflection spectroscopy measurement shows that 3-APy treatment reduce the surface recombination velocity from 1.9×10^3 cm/s to 0.2×10^3 cm/s. Surface treatment with 3-APy can create an electric field at the surface of perovskite layer to reduce surface charge and enhance charge extraction, by generating iodine vacancies in the surface region. The 3-APy drastically smooths out surface potential and suppresses the surface potential variations.

Regulation of surface potential reduces the work function and induces n-type doping on the perovskite surface by reducing the formation energy of charged iodine vacancies. Under continuous light illumination at about 55 °C in ambient air, 3-APy treated PSCs shown about 87% of initial PCE after 2,428 h, compared with control PSCs of 76% after 1368h. Under 1.2-sun continuous illumination in N2 at 65 °C, 3-APy treated PSCs retained 90% of initial PCE after 1315 h, and retained 94% of its initial PCE after 850 h at 85 °C, in 85% relative humidity.

Organometallic-functionalized interfaces: The ferrocenyl-bis-thiophene-2-carboxylate ($FcTc_2$) can react with halide perovskite as a organometallic compound, forming an organometallic functionalized interface that increases the PCE and stability of inverted solar cell devices [4]. The functionalization of the perovskite layer interface is achieved through the interaction of carboxylate and thiophene groups in $FcTc_2$ with the perovskite. $FcTc_2$ can reduce surface trap states by strong chemical Pb-O binding, and accelerated interfacial electron transfer due to the

electron-rich and electron-delocalizable ferrocene units. The strong interaction between $FcTc_2$ and perovskite contributes to the surface defects passivation and the stability of surface components [13]. $FcTc_2$ suppresses the volatilization and migration of MA^+ and I^- in perovskite by inhibiting the formation of additional bonding for enhancing device stability. Under continuous 1-sun illumination in an N_2, $FcTc_2$ treated PSCs retained >98% after 1500 h, compared with the control PSCs retaining PCE of 70%. The unencapsulated $FcTc_2$ treated PSCs retain 98% of initial PCE after 2000 h under an ambient environment or 1500 h under continuous heating, compared with control PSCs retaining <80% of the initial PCE. $FcTc_2$ treated PSCs shows >95% after 1000 h at the test of 85°C and 85% RH. The test of the cycle shocks of cold (−40°C) and heat (85°C) shown that $FcTc_2$ treated PSCs retain 85% of initial PCE after 200 cycles compared with 40% PCE of control PSCs

Using KPFM, the measurement of the surface potential of perovskite film show the impact of $FcTc_2$ on the electrical properties of the perovskite film, as shown in fig. 2(b). The interface functionalization of $FcTc_2$ has boosted device efficiency to 25.0%, with V_{OC} increasing from 1.13 V to 1.18 V. The non-radiative recombination-induced V_{OC} loss has been reduced to 363 mV, by utilizing balance theory for a quantitative analysis of photovoltage losses. The surface potential gradient has reduced from around 250 mV to approximately 150 mV, suggesting a more uniform distribution of surface potential across the film. A uniform surface potential distribution can effectively facilitate the extraction of charge carriers at the interface and suppress recombination, which was verified by the carrier kinetics characterization. $FcTc_2$ provides a uniform and stable surface component distribution to prevent surface ions from migration.

Interface engineering: Mariotti et al. effectively improved the band alignment and charge extraction at the interface between perovskite and electron transport layer, and single-junction

perovskite solar cells exhibited an open-circuit voltage of 1.28 V, as shown in Fig. 2(c). The positive dipole can be induced by the ionic liquid piperazine iodide (PI), significantly reduces non-radiative recombination losses [5]. Figure 2(c) shows the sketched band bending of interface between perovskite layer and C_{60} layer with and without PI treatment. The conduction band offset (ΔE_C) of interface is –0.31 eV. The transient surface photovoltage (trSPV) measurement showed a substantially reduced SPV signal for PI-treated films, indicating electrons transfer to the surface with excess free holes remaining in the bulk. The deficiency of surface electron concentration in perovskites raised the valence band maximum (VBM) by 200 meV, showing a higher n-type characteristic at the surface. Optimizing the perovskite composition and additive concentration has increased the V_{OC} of single-junction solar cells to 1.28 V. The V_{OC} losses have been reduced to 400 mV. Ultraviolet Photoelectron Spectroscopy (UPS) reveals that the work function of the PI-treated surface is 4.60 eV, increasing 0.14 eV compared to control film. It can be inferred that the positive dipole induced by PI alters the work function, shifts the energy levels of the electron transport layer C_{60}, decreases the conduction band, leading to an increased V_{OC}. Additive passivation reduces non-radiative recombination at the perovskite layer or perovskite-charge transport layer interface, improving V_{OC} and stability of device.

The PI can improve both stability and efficiency of single and tandem PSCs, by reducing recombination losses. The light-cycling test at 25 °C in N_2 for 1020 h shown that PI treated PSCs retain 85.03% of initial PCE, better than 81.91% of control device. The PI treated tandem PSCs retained 99.6% of initial PCE after 3000 h in N_2, and remain 80% of initial PCE after 347 h and 75.7% of initial PCE after 478 h in air at 23° to 32°C.

Potential barrier regulation in hole-transport-layer-free perovskite solar cells. Perovskite devices without hole transport layers can significantly reduce material and device

fabrication costs, shortening manufacturing time [14]. However, the perovskite films by blade coating show non-uniform surface morphology, reducing device efficiency. Wu et al. fabricated hole-transport-layer-free (HTL) PSCs by doping with 2,3,5,6-tetrafluoro-7,7,8,8-tetracyanoquinodimethane (F4TCNQ) [14]. As a strong electron-withdrawing molecule, F4TCNQ can induce band bending at the interface, promoting interfacial extraction between the perovskite layer and indium tin oxide (ITO) layer. This molecular doping strategy enabled HTL-free PSCs with over 20.0% efficiency.

KPFM measurements of the F4TCNQ-induced surface potential change on perovskite films are shown in Figure 3(a). F4TCNQ improved the efficiency of HTL-free devices to 20.2%, increasing V_{OC} from 1 V to 1.1 V. F4TCNQ lowered the surface potential of the films, enhancing the work function, indicating p-type doping. Figure 3(b) displays the impact of F4TCNQ on the band alignment at the contact interface between the perovskite layer and ITO. For undoped perovskite layers, the lower Fermi level compared to ITO (-4.7 eV) results in downward band bending of the perovskite after contact, increasing the hole extraction barrier and recombination probability. F4TCNQ increases the work function of the perovskite by around 0.2 eV, indicating more p-type character at the perovskite/ITO interface. This molecular doping induces upward band bending at the interface, lowering series resistance and extraction barriers, facilitating interfacial hole transport. The stability test shown that the unencapsulated HTL-free PSCs retain 92% of initial PCE after 500 h under ambient conditions, at 25 °C in humidity of about 20%.

Potential barrier regulation in n-i-p single-junction perovskite solar cells. The heterojunction interface between the perovskite layer and charge transport layer is crucial for interfacial charge injection and extraction dynamics. Surface defect passivation can optimize the heterojunction interface and enhance device efficiency and stability. However, surface treatment

may alter the interfacial energy, inducing a negative work function shift on the perovskite surface. In a potential well, the negative work function change (ΔW) can accumulates charges, activating halide migration and decreasing stability of device [6, 15]. The surface passivation needs to trade-off between the beneficial effect on device efficiency and detrimental effects on device stability, for improving PSC stability.

KPFM measurements indicate that the octylammonium iodide (OAI) treatment reduced the average work function from 4.67 to 4.49 eV, as shown in Fig. 4(a). The potential well induced by the negative ΔW can capture charges at the heterojunction interface, leading to charge accumulation at the interface. Cross-sectional KPFM measurements revealed significant electron accumulation at the heterojunction in OAI-treated devices, while OATsO treatment avoided electron accumulation, as shown in Fig. 4(b). An ideal photovoltaic device should have a uniform electric field distribution in the cross-section without carrier accumulation at the interface [16]. In Fig. 4(c) shows OATsO-treated devices show the efficiency of 24.41%, which was the highest among OATsO-treated devices, $OABF_4$-treated devices, and OAI-treated devices. The faster degradation of OAI-treated devices indicates accelerated ion migration due to the negative ΔW. OATsO-treated devices exhibited better stability, also suggesting modulated ion migration energetics. By tuning the counter anions to modulate the surface energy of perovskite films, both improving the uniformity of surface potential and optimizing the negative ΔW, an effective approach is provided to enhance device performance and stability.

The working mechanisms of p-type dopant molecules can be understood through the energy-level alignment of perovskite film formation on ITO [17]. A well-matched p-perovskite/ITO contact can be fabricated using a dimethylacridine-based molecular doping method with a certified PCE of 25.39%. In Figure 4c, there is a much lower ΔE_h of 0.21 eV due to the stronger p-type and

deeper Fermi level. Thus, the energy band shows an upward bend, and the hole extraction rate increases at the interface.

Reducing the negative ΔW can accumulates charges in a potential well, and lowers the halide migration activation energy for limit the stability of PSCs. OATsO treated PSCs retain its initial PCE after 800 h, $OABF_4$ treated PSCs retain 91.5% of initial PCE after 500 h, OAI-treated retain 84.8% of initial PCE after 500 h, and control PSCs retain 70% of initial PCE after 200 h, in the ambient atmosphere at about 40 °C, in 40% relative humidity. Under OC condition testing in the ambient atmosphere at about 40 °C, in 40% relative humidity, The PSCs retained 94.3% (OATsO treated), 86.2% ($OABF_4$ treated), 74.8% (OAI treated) of PCEs after 1014 h, while the control PSCs retained 50% of PCEs after 500 h. Then The PSCs retained 87.0% (OATsO treated), 65% (OAI treated) of PCEs after 2092 h. The most stable OATsO-treated PSC retained 94.9% and 88.5% of its initial PCE after 1014 h and 2092 h, respectively.

The challenges ahead in the future. In this review, we summarize that homogenizing the surface potential of the perovskite layer can improve PSCs, modulating the magnitude of the perovskite layer's surface potential helps reduce interfacial barriers and enhance charge injection efficiency in devices. Further studies are needed to understand the underlying mechanisms of surface potential on recombination losses and carrier transport in devices.

1. Further investigation of the influence of uniform surface potential distribution of perovskites on interfacial barriers. How surface potential uniformity reduce interfacial recombination and enhance carrier injection

2. The relationship between external electric field or polarization and junction/interface Schottky barrier height should be investigated through cross-sectional surface potential distribution characterized by KPFM.

3. Experiments have shown that chemical methods such as doping, adding interlayers, can effectively tune the surface potential distribution or interfacial charge transfer. It remains to be explored whether electric field modulation is a viable and effective approach to regulate interfacial barriers and enhance device performance.

4. Polarization induced by external electric fields can promote device performance through precise control of barriers, thereby contributing to future low-cost scalable manufacturing, needs to be explored.

FIGURES

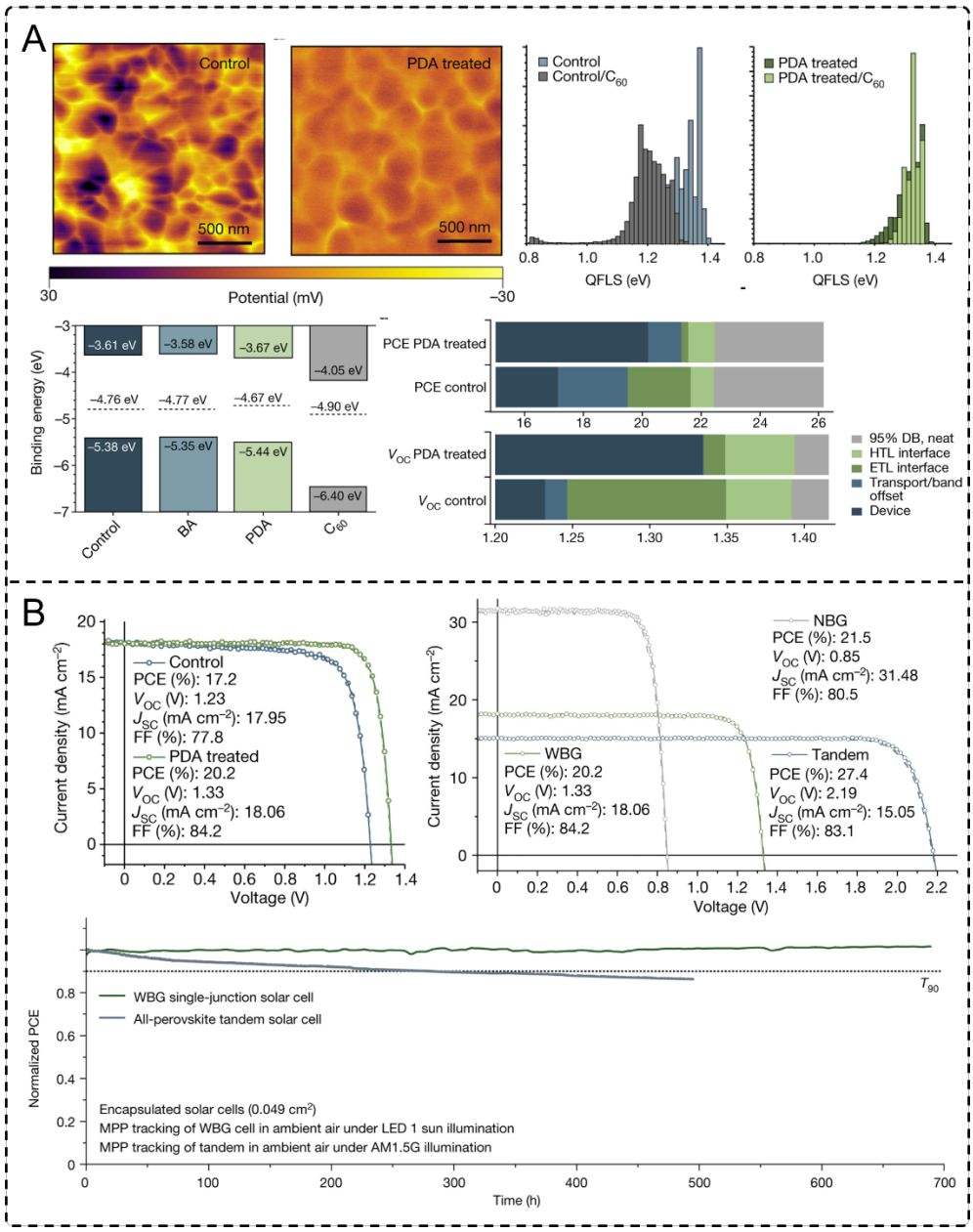

Figure 1. (a) KPFM images, histograms of QFLS, band alignment for control and PDA-treated films, loss analysis for PCE and V_{OC} of devices with control and PDA-treatment. Reproduced with permission from ref [7]. Copyright [2022] [Springer Nature]. (b) J–V curves of NBG, WBG and all-perovskite tandem devices, and stability measurement of WBG and all-perovskite tandem devices. Reproduced with permission from ref [7]. Copyright [2022] [Springer Nature].

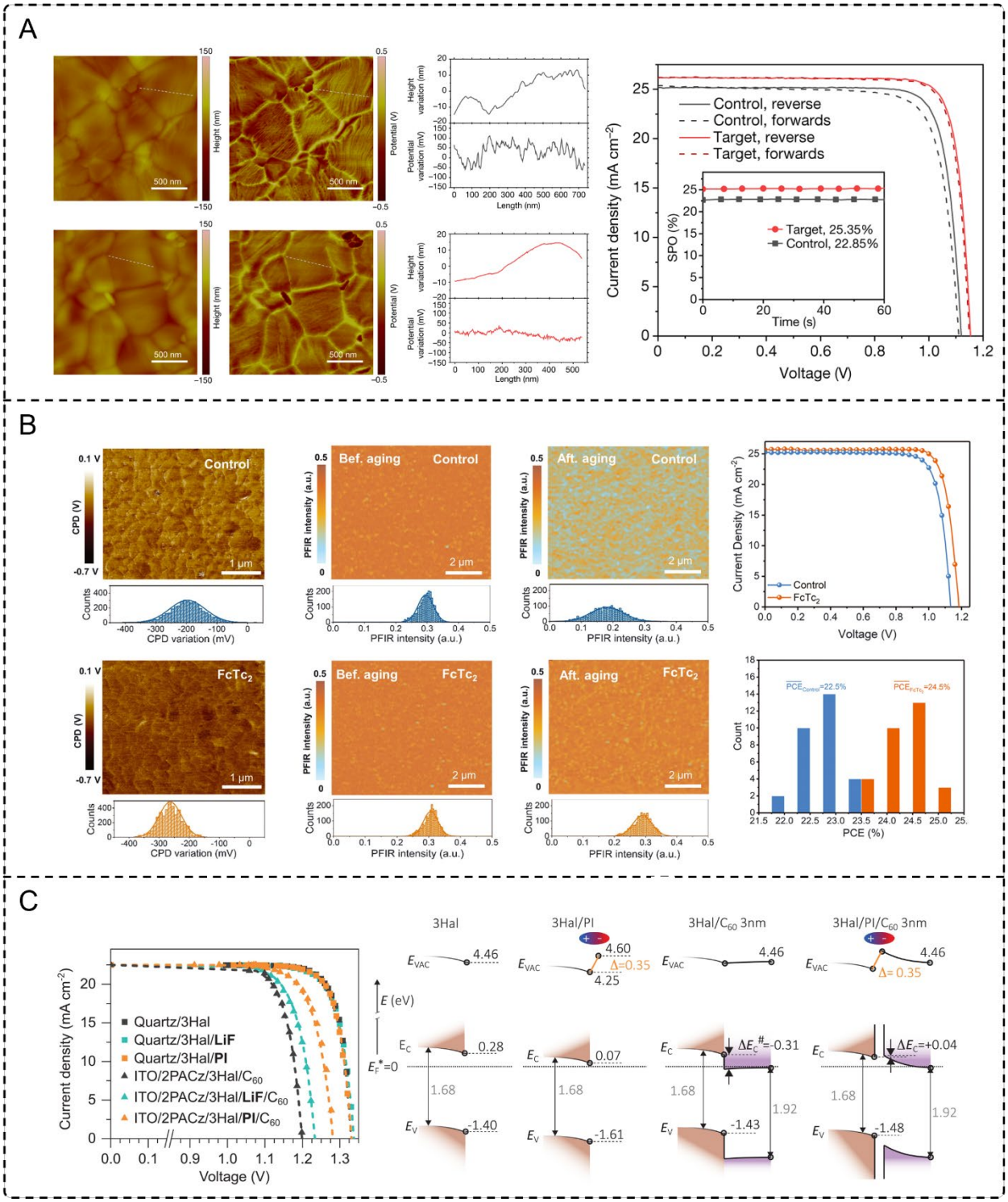

Figure 2. (a) KPFM data, J-V measurement of control and target device. Reproduced with permission from ref [3]. Copyright [2022] [Springer Nature]. (b) Surface potential images

measured by KPFM, J-V curves and histogram of the PCE data with and without $FcTc_2$. Reproduced with permission from ref [4]. Copyright [2022] [American Association for the Advancement of Science]. (c) J-V curves of device, and Energy-level alignment of different interface. Reproduced with permission from ref [5]. Copyright [2023] [American Association for the Advancement of Science].

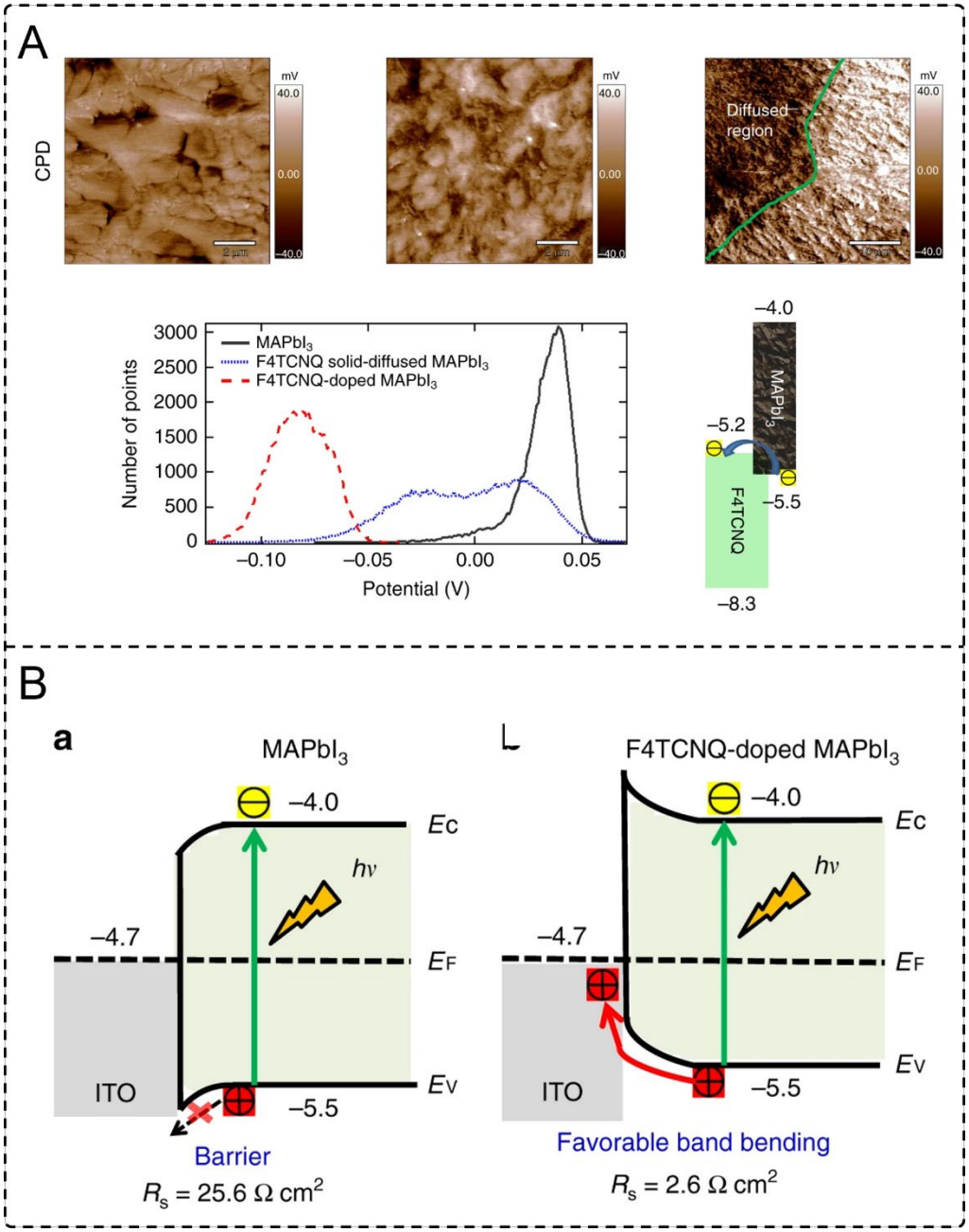

Figure 3. (a) KPFM images of films with and without F4TCNQ, schematic of the energy diagram of interface between perovskite and F4TCNQ layer. Reproduced with permission from ref [14]. Copyright [2018] [Springer Nature]. (b) Schematic of interfacial hole transfer dynamics. Reproduced with permission from ref [14]. Copyright [2018] [Springer Nature].

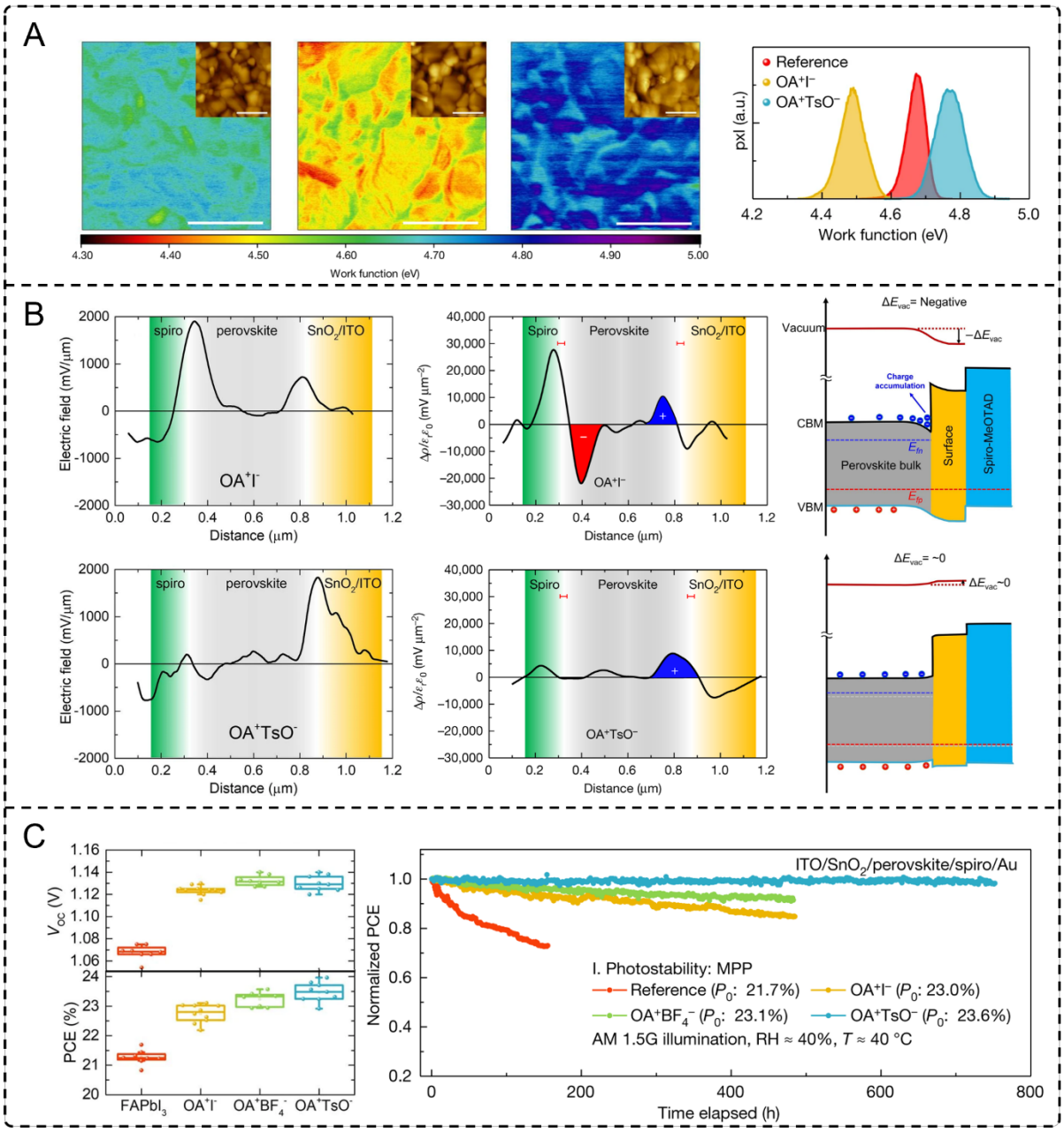

Figure 4. (a) Surface potential maps, work function distributions of reference, OAI-treated and OATsO-treated devices. Reproduced with permission from ref [6]. Copyright [2022] [Springer Nature]. (b)The electric field distribution, charge density distribution, and band diagrams of OAI-treated and OATsO-treated devices. Reproduced with permission from ref [6]. Copyright [2022] [Springer Nature]. (c) the PCE and stability measurement of devices with OAI-treated and OATsO-treated. Reproduced with permission from ref [6]. Copyright [2022] [Springer Nature].

AUTHOR INFORMATION

Corresponding Author

***Yan Zhang -** *School of Physics, University of Electronic Science and Technology of China, Chengdu 610054, China*；https://orcid.org/0000-0002-7329-0382**.** Email: zhangyan@uestc.edu.cn

Authors:

Jiaheng Nie email address: njh@cuit.edu.cn

Yaming Zhang email address: zhangyam@std.uestc.edu.cn

Jizheng Wang email address: jizheng@iccas.ac.cn

Lijie Li email address: L.Li@swansea.ac.uk

Yan Zhang email address: zhangyan@uestc.edu.cn

ACKNOWLEDGMENT

The authors are thankful for support from Major Program of National Natural Science Foundation of China (Grant No. 52192610, 52192612) and Key Program of National Natural Science Foundation of China (Grant No. U22A2077). The authors are thankful for the support by the Fundamental Research Funds for the Central Universities (grant no. ZYGX2021YGCX001).

Views expressed in this Viewpoint are those of the authors and not necessarily the views of the ACS. The authors declare no competing financial interest.

REFERENCES

(1) Liang, Z.; Zhang, Y.; Xu, H.; Chen, W.; Liu, B.; Zhang, J.; Zhang, H.; Wang, Z.; Kang, D.-H.; Zeng, J.; Gao, X.; Wang, Q.; Hu, H.; Zhou, H.; Cai, X.; Tian, X.; Reiss, P.; Xu, B.; Kirchartz, T.; Xiao, Z.; Dai, S.; Park, N.-G.; Ye, J.; Pan, X., Homogenizing out-of-plane cation composition in perovskite solar cells. *Nature* **2023,** *624* (7992), 557-563.

(2) Aydin, E.; Ugur, E.; Yildirim, B. K.; Allen, T. G.; Dally, P.; Razzaq, A.; Cao, F.; Xu, L.; Vishal, B.; Yazmaciyan, A.; Said, A. A.; Zhumagali, S.; Azmi, R.; Babics, M.; Fell, A.; Xiao, C.; De Wolf, S., Enhanced optoelectronic coupling for perovskite/silicon tandem solar cells. *Nature* **2023,** *623* (7988), 732-738.

(3) Jiang, Q.; Tong, J.; Xian, Y.; Kerner, R. A.; Dunfield, S. P.; Xiao, C.; Scheidt, R. A.; Kuciauskas, D.; Wang, X.; Hautzinger, M. P.; Tirawat, R.; Beard, M. C.; Fenning, D. P.; Berry, J. J.; Larson, B. W.; Yan, Y.; Zhu, K., Surface reaction for efficient and stable inverted perovskite solar cells. *Nature* **2022,** *611* (7935), 278-283.

(4) Li, Z.; Li, B.; Wu, X.; Sheppard, S. A.; Zhang, S.; Gao, D.; Long, N. J.; Zhu, Z., Organometallic-functionalized interfaces for highly efficient inverted perovskite solar cells. *Science* **2022,** *376* (6591), 416-420.

(5) Mariotti, S.; Köhnen, E.; Scheler, F.; Sveinbjörnsson, K.; Zimmermann, L.; Piot, M.; Yang, F.; Li, B.; Warby, J.; Musiienko, A.; Menzel, D.; Lang, F.; Keßler, S.; Levine, I.; Mantione, D.; Al-Ashouri, A.; Härtel, M. S.; Xu, K.; Cruz, A.; Kurpiers, J.; Wagner, P.; Köbler, H.; Li, J.; Magomedov, A.; Mecerreyes, D.; Unger, E.; Abate, A.; Stolterfoht, M.; Stannowski, B.; Schlatmann, R.; Korte, L.; Albrecht, S., Interface engineering for high-performance, triple-halide perovskite–silicon tandem solar cells. *Science* **2023,** *381* (6653), 63-69.

(6) Tan, S.; Huang, T.; Yavuz, I.; Wang, R.; Yoon, T. W.; Xu, M.; Xing, Q.; Park, K.; Lee, D.-K.; Chen, C.-H.; Zheng, R.; Yoon, T.; Zhao, Y.; Wang, H.-C.; Meng, D.; Xue, J.; Song, Y. J.; Pan, X.; Park, N.-G.; Lee, J.-W.; Yang, Y., Stability-limiting heterointerfaces of perovskite photovoltaics. *Nature* **2022,** *605* (7909), 268-273.

(7) Chen, H.; Maxwell, A.; Li, C.; Teale, S.; Chen, B.; Zhu, T.; Ugur, E.; Harrison, G.; Grater, L.; Wang, J.; Wang, Z.; Zeng, L.; Park, S. M.; Chen, L.; Serles, P.; Awni, R. A.; Subedi, B.; Zheng, X.; Xiao, C.; Podraza, N. J.; Filleter, T.; Liu, C.; Yang, Y.; Luther, J. M.; De Wolf, S.; Kanatzidis, M. G.; Yan, Y.; Sargent, E. H., Regulating surface potential maximizes voltage in all-perovskite tandems. *Nature* **2022,** *613* (7945), 676-681.

(8) Li, X.; Zhang, W.; Guo, X.; Lu, C.; Wei, J.; Fang, J., Constructing heterojunctions by surface sulfidation for efficient inverted perovskite solar cells. *Science* **2022,** *375* (6579), 434-437.

(9) Azmi, R.; Ugur, E.; Seitkhan, A.; Aljamaan, F.; Subbiah, A. S.; Liu, J.; Harrison, G. T.; Nugraha, M. I.; Eswaran, M. K.; Babics, M.; Chen, Y.; Xu, F.; Allen, T. G.; Rehman, A. u.; Wang, C.-L.; Anthopoulos, T. D.; Schwingenschlögl, U.; De Bastiani, M.; Aydin, E.; De Wolf, S., Damp heat–stable perovskite solar cells with tailored-dimensionality 2D/3D heterojunctions. *Science* **2022,** *376* (6588), 73-77.

(10) Abere, A.; Glunz, S.; Warta, W., Field effect passivation of high efficiency silicon solar cells. *Sol. Energ. Mat. and Sol. C.* **1993,** *29* (2), 175-182.

(11) Jang, Y.-W.; Lee, S.; Yeom, K. M.; Jeong, K.; Choi, K.; Choi, M.; Noh, J. H., Intact 2D/3D halide junction perovskite solar cells via solid-phase in-plane growth. *Nat. Energy* **2021,** *6* (1), 63-71.

(12) Saidaminov, M. I.; Williams, K.; Wei, M.; Johnston, A.; Quintero-Bermudez, R.; Vafaie, M.; Pina, J. M.; Proppe, A. H.; Hou, Y.; Walters, G.; Kelley, S. O.; Tisdale, W. A.; Sargent, E. H., Multi-cation perovskites prevent carrier reflection from grain surfaces. *Nat. Mater.* **2020,** *19* (4), 412-418.

(13) Bi, D.; Tress, W.; Dar, M. I.; Gao, P.; Luo, J.; Renevier, C.; Schenk, K.; Abate, A.; Giordano, F.; Correa Baena, J.-P.; Decoppet, J.-D.; Zakeeruddin, S. M.; Nazeeruddin, M. K.; Grätzel, M.; Hagfeldt, A., Efficient luminescent solar cells based on tailored mixed-cation perovskites. *Sci. Adv.* **2016,** *2* (1), e1501170.

(14) Wu, W.-Q.; Wang, Q.; Fang, Y.; Shao, Y.; Tang, S.; Deng, Y.; Lu, H.; Liu, Y.; Li, T.; Yang, Z.; Gruverman, A.; Huang, J., Molecular doping enabled scalable blading of efficient hole-transport-layer-free perovskite solar cells. *Nat. Commun.* **2018,** *9* (1), 1-8.

(15) Lee, J.-W.; Tan, S.; Seok, S. I.; Yang, Y.; Park, N.-G., Rethinking the A cation in halide perovskites. *Science* **2022,** *375* (6583), eabj1186.

(16) Söderström, T.; Haug, F. J.; Terrazzoni-Daudrix, V.; Ballif, C., Optimization of amorphous silicon thin film solar cells for flexible photovoltaics. *J Appl. Phys.* **2008,** *103* (11), 114509.

(17) Tan, Q.; Li, Z.; Luo, G.; Zhang, X.; Che, B.; Chen, G.; Gao, H.; He, D.; Ma, G.; Wang, J.; Xiu, J.; Yi, H.; Chen, T.; He, Z., Inverted perovskite solar cells using dimethylacridine-based dopants. *Nature* **2023,** *620* (7974), 545-551.